Letter to the Editor

Liver Langerhans cell histiocytosis in a pediatric patient: a case description and literature analysis

Tongtong Guo, Hongchang Luo

Department of Medical Ultrasound, Tongji Hospital affiliated to Tongji Medical College of Huazhong University of Science and Technology, Wuhan, China

Correspondence to: Hongchang Luo, PhD. Department of Medical Ultrasound, Tongji Hospital affiliated to Tongji Medical College of Huazhong University of Science and Technology, 1095 Jiefang Avenue, Wuhan 430030, China. Email: hongchangluo@qq.com.

Submitted Jun 20, 2023. Accepted for publication Oct 24, 2023. Published online Nov 02, 2023.
doi: 10.21037/qims-23-896
View this article at: https://dx.doi.org/10.21037/qims-23-896

Introduction

Langerhans cell histiocytosis (LCH) is an inflammatory neoplasia of myeloid precursor cells driven by mutations in the mitogen-activated protein kinase pathway. Clinically, its presentation and subsequent progress of disease may vary widely, from a single-system disease that resolves spontaneously to a refractory multisystem disease with a mortality rate of up to 20% (1,2). It usually occurs in the skeletal system, and its emergence is followed by the invasion in the cutaneous system. Liver-specific lesions are rarely reported. The definitive diagnosis of LCH is mainly based on histopathology and related immunohistochemical markers (CD1a/Langerin/S100) (3). LCH is easily misdiagnosed due to its intricate clinic features and laboratory results (4). In this report, we describe the gray-scale ultrasound and contrast-enhanced ultrasound (CEUS) features of this case for further understanding of the disease.

Case presentation

An 11-year-old girl was admitted to our hospital for treatment of unexplained abdominal pains. While hospitalized, the patient successively underwent complete laboratory examinations, as detailed in *Table 1*. The patient had no current or prior history of hepatitis B or C virus infection. Tumor markers including alpha-fetoprotein (AFP), carcinoembryonic antigen (CEA), and carbohydrate antigen 19-9 (CA19-9) were negative, as were autoantibodies including antinuclear antibody (ANA), antibodies to extractable nuclear antigens (ENAs), and antineutrophil cytoplasmic antibodies (ANCAs). During the liver function test, the levels of transaminase and bile pigment were normal, but the level of globulin was high, especially immunoglobulin G (IgG; 20.9 g/L). Of particular note, the white blood cell count (WBC) was 4.30×10^9/L. Blood cytokine levels were elevated, especially for the interleukin 2 (IL-2) receptor (1,028 U/mL), IL-8 (229 pg/mL), and tumor necrosis factor α (TNF-α; 24 pg/mL). The patient was considered to be at risk of infection, and a bacteriological inspection was performed. Heart-and-liver-protecting therapy (creatine phosphate sodium and magnesium isoglycyrrhizinate), rehydration, and other types symptomatic support therapy were carried out. The anaerobic culture (liver tissue) results were negative, which indicated that there was no significant bacterial growth, and no *Haemophilus* culture.

On the same day, the patient received a magnetic resonance imaging (MRI) examination. Multiple nodules of different sizes were scattered throughout the liver, with the largest one being about 15 mm × 11 mm in size. All nodules showed slightly longer T2-weighted signals. Most of the nodules had blurred edges and high signal in T2-weighted imaging (*Figure 1A*), limited diffusion in diffusion-weighted imaging (*Figure 1B*), and uneven enhancement in the arterial phase of perfusion-weighted imaging, with predominantly peripheral enhancement. MRI indicated multiple nodules in the liver as potentially inflammatory or infectious lesions with slightly thickened intrahepatic bile walls.

Table 1 Basic laboratory examination results from the patient

Laboratory examination	Results
Tumor marker	
AFP	(–): 1.52 ng/mL
CEA	(–): 2.11 ng/mL
CA19-9	(–): 29.72 U/mL
Autoantibody	
ANA	(–)
ENAs	(–)
ANCAs	(–)
Liver function	
IgG	20.9 g/L
IgA	2.83 g/L
Other examination	
WBC	4.30×10^9/L
IL-2 receptor	1,028 U/mL
IL-8	229 pg/mL
TNF-α	24 pg/mL

AFP, alpha-fetoprotein; CEA, carcinoembryonic antigen; CA19-9, carbohydrate antigen 19-9; ANA, antinuclear antibody; ENA, antibody to extractable nuclear antigen; ANCA, antineutrophil cytoplasmic antibody; IgG, immunoglobulin G; IgA, immunoglobulin A; WBC, white blood cell count; IL-2, interleukin 2; IL-8 interleukin 8; TNF-α tumor necrosis factor α.

After admission, the patient underwent abdominal gray-scale ultrasound and CEUS examination with an RS80A Ultrasound Machine (Samsung Medison Co., Ltd., Seoul, Korea). Gray-scale ultrasound revealed the presence of multiple hypoechoic nodules in the liver (*Figure 2A*), which were accompanied by anechoic areas mainly located in the subcapsular and apical areas of the liver, measuring 1.9 cm × 1.6 cm and 2.0 cm × 1.7 cm in size, respectively. A color Doppler flow imaging examination did not indicate blood flow in the nodule. CEUS examination was used to more deeply explore the nature of these nodules. The level of low mechanical index was 0.24. Sonovue (Bracco, Milan, Italy), a contrast agent, was mixed with 5 mL of normal saline, and then 2 mL of the mixture was injected into the patient's elbow vein. The arterial phase of CEUS examination showed mainly marginal enhancement in the abovementioned intrahepatic hyperechoic region (*Figure 2B*), with little contrast being visible in the interior of the nodule. The portal vein phase showed low enhancement in the hepatic hyperechoic region (*Figure 2C*). In the parenchymal phase, the hyperechoic region in the liver included a lower enhancement (*Figure 2D*). Quantitative CEUS parameters reflecting tissue vascularity can be obtained from time-intensity curve (TIC) analysis. The GE NUK software (NovoUltrasound Kit, GE HealthCare PDx, Chicago, IL, USA) was used to acquire the fitted TIC of a region of interest (*Figure 3A*). Quantitative analysis of CEUS showed that the contrast arrival time for the lesion was 5 s, the fall time for the lesion was 10 s, the mean transit time for the lesion was 7 s, the time to peak for the lesion was 18 s, and the time to peak for the surrounding liver tissue was 25 s. Obviously, the peak intensity of the lesion was higher than that of the surrounding liver tissue (*Figure 3B*). The CEUS findings indicated that the liver lesions did not resemble benign nodules but failed to clarify the specific nature. In general, ultrasound examination demonstrated multiple solid lesions possibly originating from infection in the liver.

Taking full consideration of the medical record and the preceding treatment, the physician recommended a hepatic biopsy to determine the nature of the liver nodule. The highly enhanced tissue, including the edges and interior of the nodules, was taken and prepared during the CEUS examination. The damaged local liver structure was found microscopically, with significant eosinophil infiltration and scattered inflammatory cells (*Figure 4*). Finally, immunohistochemical results showed the following: Langerin (+), S-100 (+), CD1α (+), CD45-leukocyte common antigen (LCA) (+), CD68 (+), CD163 (+), cyclin D1 (+), BRAF (positive control) (+), and Ki-67 labeling index about 20%. These results were consistent with LCH manifestation. Additionally, results of electron microscopy from laboratories at other hospitals also suggested LCH diagnosis although typical Birbeck granules were not found in the obtained tissue (*Figure 5*).

The treatment team conducted extensive examinations to find other invasive nodules. Bone puncture examination and a radionuclide comprehensive bone scan were also carried out. The bone puncture examination revealed active granulocyte hyperplasia and massive eosinophils. The radionuclide comprehensive bone scan detected no abnormal concentration or rarefaction of radioactivity in the skeletal system. Moreover, there was no significant rash or bleeding spots on the patient's skin. Therefore, lesions were not found in the bone or skin, and so multisystem LCH was not diagnosed.

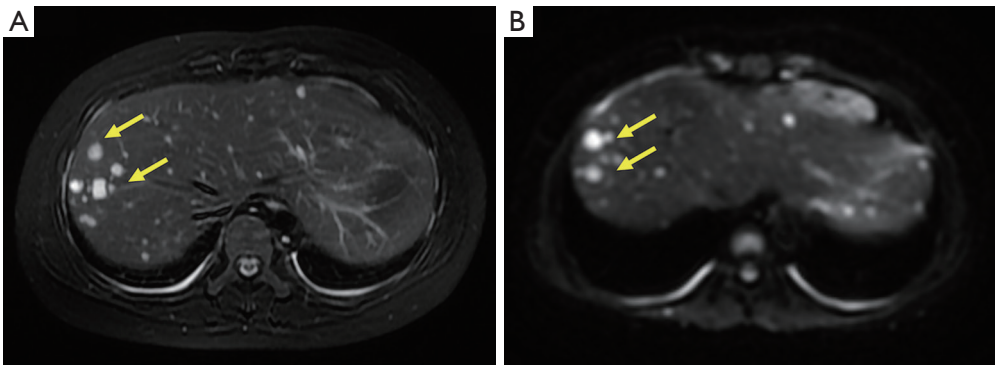

Figure 1 MRI before definitive diagnosis of the patient. Different sizes nodules were located mainly in the right lobe of the liver and subcapsule of the liver but not along the portal vein. The lesions were more obvious in MR from the macroperspective. (A) Multiple nodules with high signal in T2-weighted imaging are highlighted by yellow arrows. (B) Multiple nodules with high signal in diffusion-weighted imaging are highlighted by yellow arrows. MRI, magnetic resonance imaging; MR, magnetic resonance.

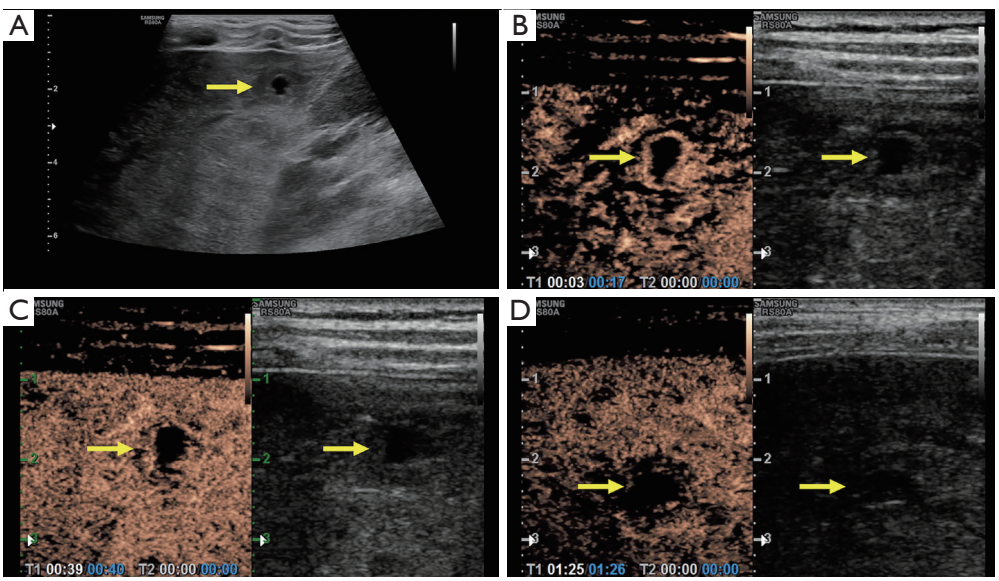

Figure 2 The imaging of ultrasound and CEUS examination, with the observed nodules being highlighted by yellow arrows. Nodules had a different appearance in different periods (A) B-mode ultrasound showing a heterogeneous hypoechoic nodule, with no echo in the center. (B) Marginal high enhancement of a nodule in the arterial phase under CEUS examination. (C) Slightly low marginal enhancement in the portal vein phase under CEUS examination. (D) Lower overall enhancement in the parenchymal phase under CEUS examination. CEUS, contrast-enhanced ultrasound.

Following this, the patient in our case was transferred from the pediatric infectious gastroenterology unit to the pediatric hematology unit. She initially underwent anti-infective therapy at our hospital and at the time of writing, is being treated with a specialized anti-LCH therapy. First-line chemotherapy (prednisolone and vinblastine sulfate) was administered successfully. Over the next half of the month, the patient was free from abdominal pain. Clinical symptoms were comprehensively alleviated, but the number and size of nodules in liver had reduced or diminished. Therefore, nonrisky second-line chemotherapy (vindesine, cytarabine, and prednisone) was administered. Smaller and fewer nodules than those encountered during first-line chemotherapy were found in the liver via MRI (*Figure 6A*,*6B*). The levels of transaminase, bile pigment, and globin returned to normal. The lymphocyte and monocyte count in routine blood

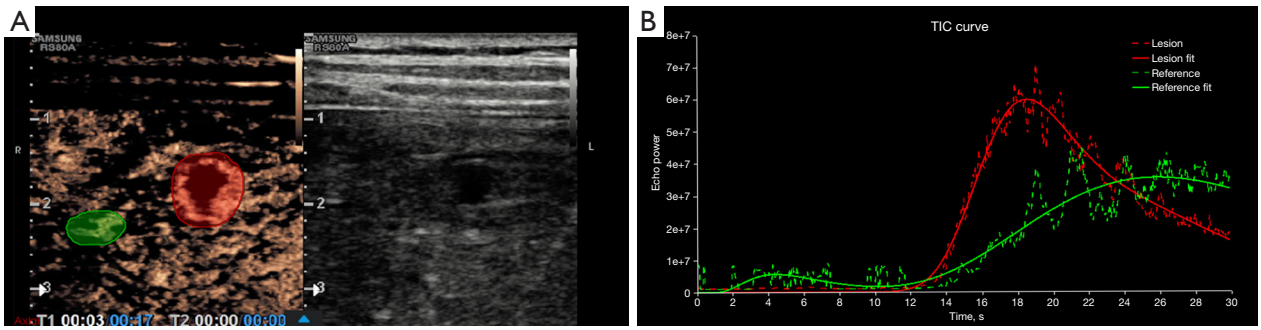

Figure 3 The TIC imaging of concrete quantitative analysis after CEUS examination. (A) With the red curve delineating the border of nodule and the green curve delineating normal liver tissue as reference, the nodule's quantitative CEUS was analyzed. (B) The nodule was rapidly enhancing and subsiding, and in contrast, the normal liver tissue was enhancing slowly over a longer period. TIC, time-intensity curve; CEUS, contrast-enhanced ultrasound.

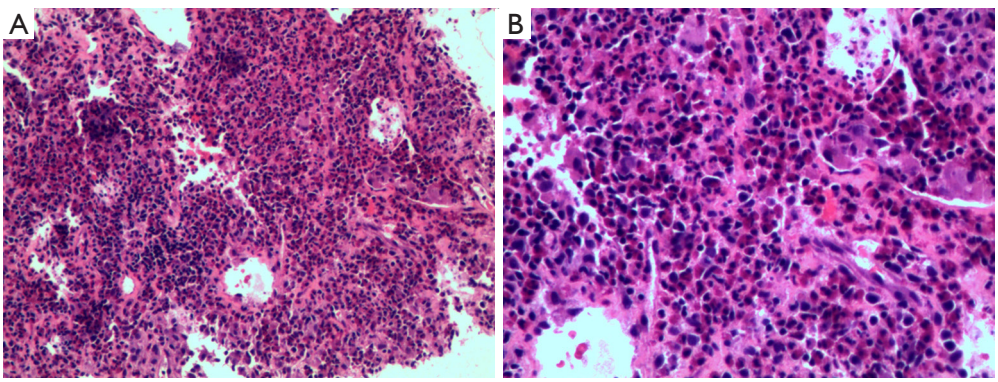

Figure 4 Histopathological diagnostic images in an 11-year-old girl with liver LCH diagnosed via ultrasound-guided biopsy. The histopathological image revealed a broken local liver structure, significant eosinophil infiltration, and scattered inflammatory cells. Hematoxylin and eosin staining at magnification ×40 (left) and ×100 (right). Immunohistochemical examination findings of Langerin (+) and S-100 (+) indicated liver LCH. LCH, Langerhans cell histiocytosis.

testing had returned to a normal range.

All procedures performed in this study were in accordance with the ethical standards of the institutional and/or national research committee(s) and with the Helsinki Declaration (as revised in 2013). Written informed consent was provided by the patient's legal guardians for publication of this case presentation and accompanying images. A copy of the written consent is available for review by the editorial office of this journal.

Discussion

LCH is a rare proliferative disease with an incidence of 2.6 to 5.4 cases per million children (5). Due to it being a multisystem disease and its intricate clinical manifestation, LCH is difficult to diagnose. Once a patient is suspected of having LCH, pathological biopsy and accurate immunohistochemical examination are essential for a definitive diagnosis (6).

Isolated-liver LCH is rare, but liver involvement is commonly found in disseminated LCH, mainly within pediatric patients (7). To our knowledge, few reports of isolated liver LCH have been published in the PubMed English-language literature. However, in reports of most patients with liver LCH, these patients were sent to hospital with hepatic lesion, extra-hepatic bile duct tumor, hepatic dysfunction, or jaundice as the first presentation, which were usually accompanied by other nodules in the bone, skin, or even the pulmonary system (4,8-10). Some researchers believe that liver LCH could progress

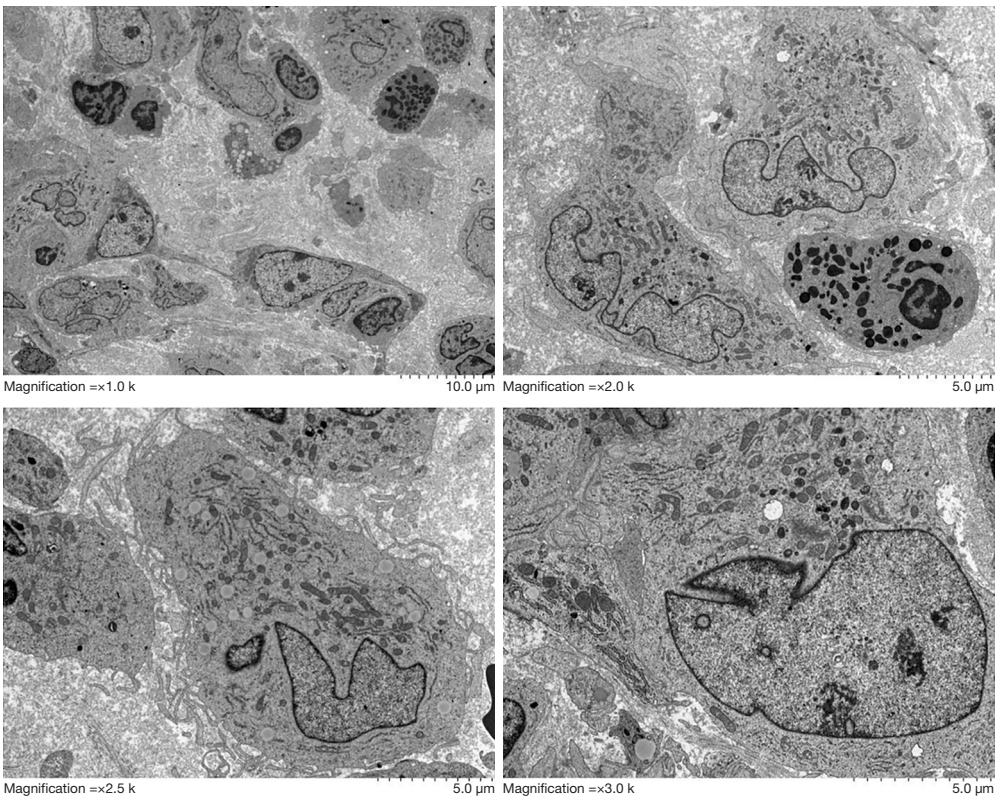

Figure 5 The results of electron microscopy from needle biopsy tissue. Liver LCH was diagnosed, but typical Birbeck granules were not found. Hematoxylin and eosin staining at magnification ×1.0 k, ×2.0 k, ×2.5 k, and ×3.0 k. The scales (10.0 µm, 5.0 µm) represent values of the entire scales. LCH, Langerhans cell histiocytosis.

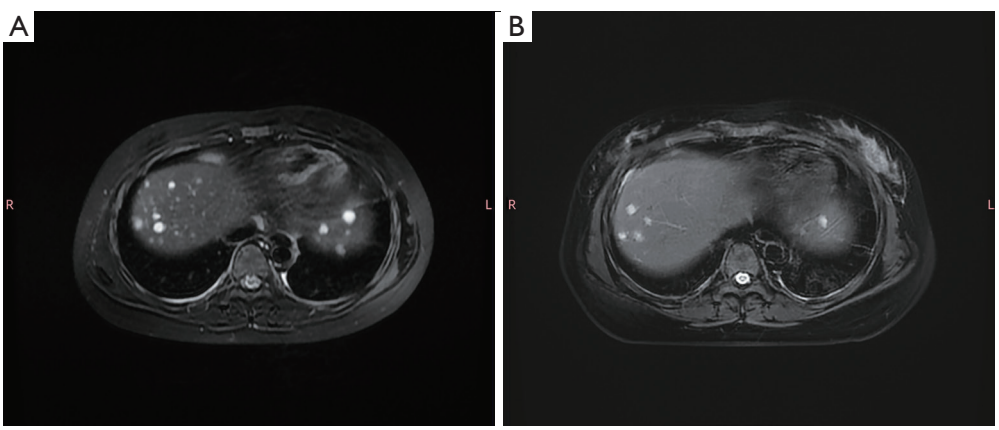

Figure 6 The MRI during the patient's treatment. (A) Many large nodules, high signal in T2-weighted imaging, a diffused distribution were found in the liver during first-line chemotherapy. (B) Smaller and fewer nodules and high signal in T2-weighted imaging were found in the liver during nonrisky second-line chemotherapy. MRI, magnetic resonance imaging; L, left; R, right.

to end-stage chronic liver disease due to its potential to develop into sclerosing cholangitis in disseminated LCH. Liver involvement in disseminated LCH indicates the late phase of LCH (11,12) and is likely to be found in the gastrointestinal tract of most affected children, traveling through the portal vein to the blood stream and ultimately

into the liver and causing infection of the biliary tract or liver parenchyma (13). In one case report, the patient had acute liver failure with cutaneous, renal, pituitary, and hematologic manifestations of secondary LCH (14). The liver transplant was the only solution for a cure. Most literature on liver LCH has been published by journals in the transplantation field. Generally, poor prognosis is often associated with late-phase LCH, particularly in adults, and orthotopic liver transplantation is often performed to improve clinical symptoms (11,12). This requires more careful care and follow-up after transplantation, resulting in a heavy burden on patients and increased social medical pressure. Therefore, the early diagnosis of liver LCH is crucial, and a convenient sonography examination will be a first choice to achieve early discovery and early screening.

For certain diseases, depending on the involved body part, ultrasound is not preferred for early detection or screening. However, without early diagnosis, scheduling of early treatment in time and a good prognosis are not possible. In one case of pulmonary LCH, thoracic computed tomography (CT) indicated multiple diffuse cystic lesions in both lungs with right pneumothorax. During pleurodesis, numerous distinctive bullae were found in the lung (15). However, such specific pathological features were not demonstrated on ultrasound. This indeed may be the case for lung or gastrointestinal tract disease (16) due to interference from gas. The ultrasound waves can barely propagate through the tissue, resulting in poor diagnostic relevance for lung or gastrointestinal tract diseases. In another case of LCH with pituitary involvement, the manifestations were heterogeneous, mainly low-signal and patchy high-signal nodules on magnetic resonance (MR) T2-weighted imaging, which suggested an inflammatory tumor-like lesion all over the body that was eventually diagnosed as LCH (17). For rare cases of brain LCH, ultrasound is also not a suitable diagnostic method, but MR is superior to CT in the diagnosis of soft tissue lesions. When the skull reaches a certain stage, the structure in the skull has been completely blocked by the skull. Because the ultrasonic wave cannot completely penetrate the skull, the structure and lesions of the brain cannot be explored; this constitutes a major limitation of ultrasound. However, when multiple liver nodules and superficial lesions, such as skin lesions, are detected by ultrasound, proper consideration should be given to a potential diagnosis of LCH without delay of treatment.

For liver LCH, ultrasound has the benefit of real-time discovery, fine resolution of the liver tissue, and economic benefits. Many imaging methods have been applied to assist the diagnosis of liver LCH, among which ultrasound has certain advantages compared with CT and MR. In previous reports, periportal nodules were typically found in the early proliferative phase, with irregular hyperecho in B-mode ultrasound, low density in CT, and low T2-weighted signal in MRI (18). In the study of Shi *et al.*, all 13 children diagnosed with liver LCH were found with band-like or nodular lesions in CT and MRI, which manifest as periportal abnormalities (19).

More importantly, the blood supply of hepatic tissue can be easily discerned and the nature of the tissue explored with CEUS examination, but this has not been extensively reported. In the reports of Chaudhary *et al.* (7) and Gupta *et al.* (20), contrast-enhanced CT examination of most nodules characteristically showed well-circumscribed hypodense hepatic nodules with ring enhancement and extensive periportal hypodense nodules. As commonly known, completing a full CT or MR examination is more costly than is ultrasound examination. However, regardless of the examination type, higher-resolution ultrasound that can visualize lesions in detail has an absolute advantage. In their report, Mampaey *et al.* (18) indicated that sonography showed complex hypoechoic nodules, with no diffuse enhancement and no periportal abnormalities such as those described in previous reports. In this case, our situation was slightly similar to that of Mampaey *et al.* compared with CT or MR, CEUS examination additionally revealed the activity of the nodules to guide needle biopsy for valuable tissue collection, facilitating a definitive diagnosis. The commonality among these previous cases was that most of the liver nodules mentioned were diagnosed via ultrasound-guided puncture. Thus, ultrasound has considerable advantages in the diagnosis of liver diseases.

Our patient described here is the first reported case in over 10 years of isolated-liver LCH initially detected via quantitative CEUS imaging. The quantitative CEUS examination was performed in this case. Due to the advantages of CEUS in high-resolution and real-time detection, hypoechoic nodules mainly featured uneven annular high enhancement, but only a small amount of contrast agent filled the center of nodules. In addition, quantitative CEUS examination revealed that the nodules were rapidly enhancing and subsiding relative to normal liver tissue. Considering the above imagological signs, we believed that the contrast agent-filled part of the lesion suggested blood supply, indicating that the central tissue might have been active, while the part without contrast agent-filled part was considered to

be necrosis, suggesting an inflammatory lesion in this case. However, after analyzing the report of the quantitative CEUS examination, we considered the nodule to be a neoplastic lesion. The nature of LCH has been debated in terms of it being neoplastic or inflammatory in origin, as these two etiologies would have different diagnostic implications (13). According to the treatment strategy of our case, LCH was consistently deemed to be a neoplastic lesion. As a result, quantitative CEUS examination might be helpful to distinguish between etiologies of neoplasm and inflammation in lesions.

From the perspective of liver LCH, the progress of histology consists of four different phases in chronological order: a proliferative phase, a granulomatous phase, a xanthomatous phase, and eventually a fibrous phase (21). Special pathology examination is the only method to accurately determine the stage of liver involvement. The improvement in our patient after chemotherapy implied that the disease might not have been in the late phase. To a certain extent, this might be explained by the fact that CEUS can predict if liver LCH is not in the late stage. However, the relevant literature (22) suggests that among patients with LCH and at-risk organ involvement, liver LCH is an independent factor for poor prognosis. This may be the reason why standard first-line chemotherapy was not effective in treating the liver LCH in our case. Furthermore, the discrepancy in the performance in ultrasound between our case and that of previous cases might be due to their different histological staging, which should be examined further in future work. Overall, to determine whether CEUS can predict the pathological stage and guide treatment planning, an analysis of a large sample of LCH cases will be needed. For patients with liver LCH, it is necessary to choose treatment according to the pathological stage, location, and number of occurrences, and then to adjust the program according to the imaging methods.

Conclusions

Early detection, early diagnosis, and early treatment of LCH, especially liver LCH, is urgently needed. Although isolated-liver involvement in LCH is rare and easily misdiagnosed, B-mode ultrasound and CEUS examination, with their unique advantages, may be beneficial in facilitating diagnosis earlier than may CT or MR. Quantitative CEUS examination is valuable for distinguishing neoplastic lesions from inflammation in liver LCH.

Acknowledgments

Funding: None.

Footnote

Conflicts of Interest: Both authors have completed the ICMJE uniform disclosure form (available at https://qims.amegroups.com/article/view/10.21037/qims-23-896/coif). The authors have no conflicts of interest to declare.

Ethical Statement: The authors are accountable for all aspects of the work in ensuring that questions related to the accuracy or integrity of any part of the work are appropriately investigated and resolved. All procedures performed in this study were in accordance with the ethical standards of the institutional and/or national research committee(s) and with the Helsinki Declaration (as revised in 2013). Written informed consent was provided by the patient's legal guardians for publication of this case presentation and accompanying images. A copy of the written consent is available for review by the editorial office of this journal.

References

1. Allen CE, Merad M, McClain KL. Langerhans-Cell Histiocytosis. N Engl J Med 2018;379:856-68.
2. Haupt R, Minkov M, Astigarraga I, Schäfer E, Nanduri V, Jubran R, Egeler RM, Janka G, Micic D, Rodriguez-Galindo C, Van Gool S, Visser J, Weitzman S, Donadieu J; . Langerhans cell histiocytosis (LCH): guidelines for diagnosis, clinical work-up, and treatment for patients till the age of 18 years. Pediatr Blood Cancer 2013;60:175-84.
3. Fu Z, Li H, Arslan ME, Ells PF, Lee H. Hepatic Langerhans cell histiocytosis: A review. World J Clin Oncol 2021;12:335-41.
4. Ma J, Jiang Y, Chen X, Gong G. Langerhans cell

histiocytosis misdiagnosed as liver cancer and pituitary tumor in an adult: A case report and brief review of the literature. Oncol Lett 2014;7:1602-4.
5. Broadbent V, Egeler RM, Nesbit ME Jr. Langerhans cell histiocytosis--clinical and epidemiological aspects. Br J Cancer Suppl 1994;23:S11-6.
6. Zhou AS, Li L, Carroll TL. Laryngeal Langerhans Cell Histiocytosis: A Case Report and Literature Review. Ann Otol Rhinol Laryngol 2021;130:429-33.
7. Chaudhary A, Debnath J, Thulkar S, Seth T, Sinha A. Imaging findings in hepatic Langerhans' cell histiocytosis. Indian J Pediatr 2006;73:1036-8.
8. Hatemi I, Baysal B, Senturk H, Behzatoglu K, Bozkurt ER, Ozbay G. Adult Langerhans cell histiocytosis and sclerosing cholangitis: a case report and review of the literature. Hepatol Int 2010;4:653-8.
9. Liu DG, Zhang YX, Li F. Multisystem Langerhans cell histiocytosis with liver dysfunction as the first presentation: A case report. Oncol Lett 2012;3:391-4.
10. Obiorah IE, Velasquez AH, Kallakury B, Özdemirli M. Primary Langerhans Cell Histiocytosis of the Extrahepatic Bile Duct Occurring in an Adult Patient. Balkan Med J 2018;35:437-9.
11. Ziogas IA, Kakos CD, Wu WK, Montenovo MI, Matsuoka LK, Zarnegar-Lumley S, Alexopoulos SP. Liver Transplantation for Langerhans Cell Histiocytosis: A US Population-Based Analysis and Systematic Review of the Literature. Liver Transpl 2021;27:1181-90.
12. Menon J, Shanmugam N, Valamparampil J, Vij M, Kumar V, Munirathnam D, Hakeem A, Rammohan A, Rela M. Outcomes of liver transplantation in children with Langerhans cell histiocytosis: Experience from a quaternary care center. Pediatr Blood Cancer 2023;70:e30024.
13. Behdad A, Owens SR. Langerhans cell histiocytosis involving the gastrointestinal tract. Arch Pathol Lab Med 2014;138:1350-2.
14. Hountondji L, Debourdeau A, Meunier L. Acute liver failure secondary to Langerhans cell histiocytosis. Clin Res Hepatol Gastroenterol 2022;46:101744.
15. Varkki S, Tergestina M, Bhonsle VS, Moses PD, Mathai J, Korula S. Isolated pulmonary Langerhans cell histiocytosis. Indian J Pediatr 2013;80:700-3.
16. Hait E, Liang M, Degar B, Glickman J, Fox VL. Gastrointestinal tract involvement in Langerhans cell histiocytosis: case report and literature review. Pediatrics 2006;118:e1593-9.
17. Ramji HF, Deng F. Langerhans Cell Histiocytosis Reactivation in a Teenager. J Pediatr 2022;248:131-2.
18. Mampaey S, Warson F, Van Hedent E, De Schepper AM. Imaging findings in Langerhans' cell histiocytosis of the liver and the spleen in an adult. Eur Radiol 1999;9:96-8.
19. Shi Y, Qiao Z, Xia C, Gong Y, Yang H, Li G, Pa M. Hepatic involvement of Langerhans cell histiocytosis in children--imaging findings of computed tomography, magnetic resonance imaging and magnetic resonance cholangiopancreatography. Pediatr Radiol 2014;44:713-8.
20. Gupta AK. Imaging findings in Langerhans cell histiocytosis involving lung and liver. Indian J Pediatr 2009;76:560-1.
21. König CW, Pfannenberg C, Trübenbach J, Remy C, Böhmer GM, Ruck P, Claussen CD. MR cholangiography in the diagnosis of sclerosing cholangitis in Langerhans' cell histiocytosis. Eur Radiol 2001;11:2516-20.
22. Wang DS, Lu MY, Yang YL, Lin DT, Lin KH, Chang HH, Jou ST. Clinical outcomes of childhood Langerhans cell histiocytosis in Taiwan: A single-center, 20-year experience. J Formos Med Assoc 2021;120:594-601.

Cite this article as: Guo T, Luo H. Liver Langerhans cell histiocytosis in a pediatric patient: a case description and literature analysis. Quant Imaging Med Surg 2024;14(1):1159-1166. doi: 10.21037/qims-23-896

